Journal Pre-proofs

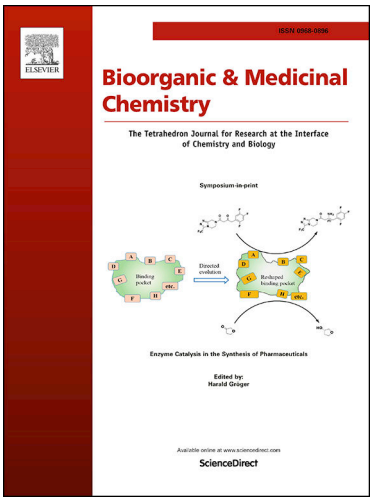

N^1-Substituted benzimidazole scaffold for farnesoid X receptor (FXR) agonists accompanying prominent selectivity against vitamin D receptor (VDR)

Arisa Masuda, Keigo Gohda, Yusuke Iguchi, Ko Fujimori, Yukiko Yamashita, Keisuke Oda, Mizuho Une, Naoki Teno

PII: S0968-0896(20)30338-2
DOI: https://doi.org/10.1016/j.bmc.2020.115512
Reference: BMC 115512

To appear in: *Bioorganic & Medicinal Chemistry*

Received Date: 26 March 2020
Revised Date: 11 April 2020
Accepted Date: 13 April 2020

Please cite this article as: A. Masuda, K. Gohda, Y. Iguchi, K. Fujimori, Y. Yamashita, K. Oda, M. Une, N. Teno, N^1-Substituted benzimidazole scaffold for farnesoid X receptor (FXR) agonists accompanying prominent selectivity against vitamin D receptor (VDR), *Bioorganic & Medicinal Chemistry* (2020), doi: https://doi.org/10.1016/j.bmc.2020.115512

N^1-Substituted benzimidazole scaffold for farnesoid X receptor (FXR) agonists accompanying prominent selectivity against vitamin D receptor (VDR)

Arisa Masuda,[a] Keigo Gohda,[b] Yusuke Iguchi,[c] Ko Fujimori,[d] Yukiko Yamashita,[c] Keisuke Oda,[c] Mizuho Une,[a,c] Naoki Teno,[a,e,*]

[a]Graduate School of Pharmaceutical Sciences, Hiroshima International University, 5-1-1 Hirokoshingai, Kure, Hiroshima 737-0112, Japan
[b]Computer-aided Molecular Modeling Research Center, Kansai (CAMM-Kansai), 3-32-302, Tsuto-Otsuka, Nishinomiya 663-8241, Japan
[c]Faculty of Pharmaceutical Sciences, Hiroshima International University, 5-1-1 Hirokoshingai, Kure, Hiroshima 737-0112, Japan
[d]Department of Pathobiochemistry, Osaka University of Pharmaceutical Sciences, 4-20-1 Nasahara, Takatsuki, Osaka 569-1094, Japan
[e]Faculty of Clinical Nutrition, Hiroshima International University, 5-1-1 Hirokoshingai, Kure, Hiroshima 737-0112, Japan

*Corresponding author:
Prof. Naoki Teno
Hiroshima International University,
Graduate School of Pharmaceutical Sciences,
5-1-1, Hirokoshingai, Kure, Hiroshima 737-0112, Japan
Tel,: +81 823 73 8593; Fax: +81 823 73 8981
e-mail: n-teno@hirokoku-u.ac.jp

Abbreviations:
FXR, Farnesoid X receptor; CDCA, Chenodeoxycholic acid; CYP7A1, Cholesterol 7α-hydroxylase; BSEP, Bile salt export pump; SHP, Small heterodimer partner; OSTα, Organic solute transporter α; CAR, Constitute androstane receptor; PXR, Pregnane X receptor; RXRα, Retinoid X receptor α; 9-*cis*-RA, 9-*cis*-Retinoic acid; 1,25-OH-VD_3, 1α,25-Dihydroxy-vitamin D_3; TGR5, Transmembrane G protein-coupled receptor 5; FGF15, Fibroblast growth factor 15; NASH, Non-alcoholic steatohepatitis; LBD, Ligand binding domain; TR-FRET, Time-resolved fluorescence resonance energy transfer; RT-PCR, Reverse transcription polymerase chain reaction; BMP-2, Bone morphogenetic protein-2; ST-2 MSCs, Mouse bone marrow-derived mesenchymal stem

cell (MSC)-like ST2 cells; GS, Guggulsterone; ALP, Alkaline phosphatase; SAR, Structure-activity relationship; Et_3N, Triethylamine; DMF, N,N-Dimethylformamide; THF, Tetrahydrofuran; Boc, *tert*-Butoxycarbonyl; HOAt, 1-Hydroxy-7-azabenzotriazole; WSCI.HCl, 1-(3-Dimethylaminopropyl)-3-ethylcarbodiimide hydrochloride; TBAF, *tetra*-*n*-Butylammonium fluoride;

Abstract

As a cellular bile acid sensor, farnesoid X receptor (FXR) participates in regulation of bile acid, lipid and glucose homeostasis, and liver protection. With respect to the bone metabolism, FXR positively regulates bone metabolism through both bone formation and resorption of the bone remodeling pathways. Some of FXR agonists possessing isoxazole moiety are undergoing clinical trials for the treatment of non-alcoholic steatohepatitis. To date, therefore, the activation of FXR leads to considerable interest in FXR as potential therapeutic targets. We have identified a series of nonsteroidal FXR agonists bearing N^1-methyl benzimidazole and isoxazole moieties that are bridged with aromatic derivatives. They showed affinity to FXR, but also weak affinity toward the vitamin D receptor (VDR) that involves regulation of calcium and phosphate homeostasis and is activated by bile acids. The deployment of FXR agonists without activity against VDR as off-target is therefore crucial in the development of FXR ligands. Our efforts focusing on increasing the agonist properties towards FXR led to the discovery of **19**, which activates FXR at and below nanomolar levels (EC_{50} = 26.5 ± 10.5 nM TR-FRET and 0.8 ± 0.2 nM luciferase, respectively) and functions as a FXR agonist: the affinity toward FXR over eight nuclear receptors, including VDR [IC_{50} (VDR) / EC_{50} (FXR) > 5000] and TGR5, effects FXR target genes, and activates bone morphogenetic protein-2-induced differentiation of mouse bone marrow-derived mesenchymal stem cell-like ST2 cells into osteoblast.

Key words

FXR agonist, Benzimidazole, Osteoblast differentiation.

1. Introduction

Nuclear hormone receptors (NHRs) are transcription factors that work in concert with coactivators and co-repressors to regulate gene expression.[1] Bile acid synthesis is under negative feedback control through activation of the nuclear receptor farnesoid X receptor (FXR, NR1H4) in the ileum and liver.[2,3] FXR and the cholesterol-sensing liver X receptor (LXR, NR1H2/3) form a complicated control network with other members of NHRs, the constitute androstane receptor (CAR, NR1I3) and the pregnane X receptor (PXR, NR1I2)[4] that function as the xenobiotic-sensing nuclear receptors in liver diseases.[5] Chenodeoxycholic acid (CDCA),[2] as an endogenous ligand of FXR, transcriptionally regulates the expression of cholesterol 7α-hydroxylase (CYP7A1) through the nuclear receptors small heterodimer partner (SHP) and the liver receptor homolog-1 (LRH-1).[6] Recent data suggest that intestinal FXR regulates hepatic CYP7A1 through a fibroblast growth factor 15 (FGF15)-dependent mechanism.[7] FXR regulates transport of proteins, the bile salt export pump (BSEP) and the organic solute transporter α (OSTα) that are involved in hepatocellular excretion.[8] With respect to the bone metabolism, bile acids enhance the differentiation of mesenchymal stem cells (MSCs) into osteoblasts though FXR.[9,10] FXR deficiency reveals a decrease in bone mineral density[11] and deletion of FXR-regulated SHP decreased bone mass through repression of osteoblast differentiation.[12] FXR agonists could activate osteoblast differentiation,[13] indicating that osteoblast differentiation is available to evaluate the activity of FXR agonist.

To date, many FXR agonists have been reported[13-30] and the most representative non-steroidal FXR agonist is GW4064 (**1**), which is composed of isoxazole and stilbene moieties.[30] (Figure 1) These portions of GW4064 (**1**) lie co-planar to each other, allowing the agonist to fit into a narrow region of the ligand binding domain (LBD) in FXR.[31] Some FXR agonists (**2-12**) possess an alternative structure to the stilbene substituent which might elicit a potentially toxic[15-17,32-37] while preserving isoxazole derivatives.[13-24] (Figure 1) From these analogs, tropifexor (**2**), a highly potent nonsteroidal FXR agonist, is undergoing clinical trials for the treatment of non-alcoholic steatohepatitis (NASH).[14,38] A partial FXR agonist (**9**) was identified by Eli Lilly.[21] Terns Pharmaceuticals licensed this compound in 2018 and TERN-101 (**9**) is in Phase 1.[38,39] Cilofexor (**10**),[40] which is analogous to **3**,[22] is also currently undergoing clinical evaluation.[38]

We have previously reported the chemotype for FXR agonists in which an isoxazole moiety[30] and N^1-substituted benzimidazole are bridged with aromatic derivatives

(**12-15**).[13] (Table 1) These analogs revealed the agonistic activity against FXR and a significant affinity with FXR toward eight nuclear receptors and transmembrane G protein-coupled receptor 5 (TGR5). In addition, we have identified that **13** and **14** activated bone morphogenetic protein-2 (BMP-2)-induced differentiation of mouse bone marrow-derived MSC-like ST2 cells (ST-2 MSCs) into osteoblasts.[13] The modeling study implied that **14** occupied the same binding pocket as GW4064; there is the possibility that LBD is not occupied by GW4064.[13] In further profiling of the activities of **12-15**, they retained a weak antagonism against the vitamin D receptor (VDR, NR1I1) at micromolar levels even though GW4064 (**1**) had no affinity with VDR. (Table 1)

Figure 1. Representative FXR agonists with isoxazole derivatives

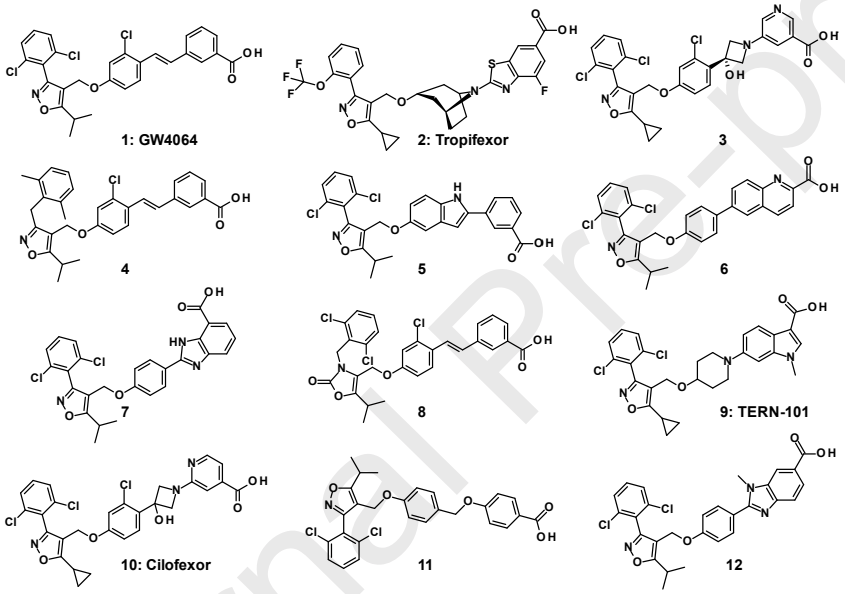

Table 1. Effects of reported analogs, **12**-**15** on FXR and VDR

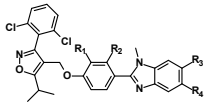

Cpds.	R_1	R_2	R_3	R_4	FXR EC_{50} (nM) TR-FRET	Relative potency (%)	FXR EC_{50} (nM) Luciferase	Relative potency (%)	VDR IC_{50} (nM) Luciferase	Relative potency (%)
1	-	-	-	-	96.2±62.7*	135.8±42.6*	13.2±13.9	102.4±8.9	>10000	47.5±7.6
12*	H	H	COOH	H	43.7±54.2*	58.2±26.2*	32.0±38.1	101±31.1	7151.3±3853.3	55.2±4.5
13*	H	H	H	COOH	64.4±135.1*	58.3±20.4*	25.8±26.0	65.6±12.2	4407.7±284.0	62.9±4.8
14*	Cl	H	COOH	H	13.4±7.9*	51.1±27.6*	19.0±17.4	64.6±8.1	2454.3±2006.5	74.2±13.6
15*	H	Cl	COOH	H	31.6±26.9*	76.4±23.4*	3.66±4.66	70.1±15.1	3519.0±716.9	81.1±0.7

*: see reference No. 22

VDR is also known as a member of the NHR1 subfamily of the NHR superfamily.[41] VDR binds 1α,25-dihydroxy-vitamin D_3 (1,25-OH-VD_3, calcitriol) with high affinity and mediates regulation of calcium and phosphate homeostasis.[42] Common feature of FXR and VDR is that both receptors are activated by bile acids as cholesterol products.[43] Indeed, docking studies suggested a common key interaction for bile acid with FXR and VDR.[43] Although the majority of the VDR ligand was based on the secosteroidal scaffold of calcitriol and recently several other non-secosteroidal VDR ligands have been reported.[44-48]

The deployment of FXR agonists without activity against VDR as off-target is crucial for future design of FXR ligands. Toward the development of the selective FXR ligands, our efforts have focused on increasing the agonistic potency against FXR based on the structures of **12-15**. The primary modeling study data[13] enabled further insight that the region not occupied by GW4064 (**1**) in LBD could be used to increase the interaction with FXR. Considering this observation, substituents extending from nitrogen atom (N^1) in benzimidazole of **12** could be appropriate for filling the vacant space in LBD of FXR. We describe herein that a structure-activity relationship (SAR) on the N^1-substituted benzimidazole of **12** was explored to identify the potent and selective FXR agonists and examine the agonism by the activation of ST-2-MCSs differentiation into osteoblasts.

2. Chemistry

Preparation of **19** is outlined in Scheme 1 as the representative example. Synthetic protocol (Schemes S1-S7) and characterizations of other analogs are available in Supplementary Data. The starting material, methyl 4-amino-3-(1-ethylpropylamino)benzoate[49] was coupled with 4-benzyloxybenzoic acid using Et_3N, HOAt and WSCI.HCl in DMF was performed to yield **19a**. Immediate ring closure of **19a** in CH_3COOH gave **19b**. After removal of benzyl group of **19b**, followed by coupling with 4-(bromomethyl)-3-(2,6-dichlorophenyl)-5-isopropyl-isoxazole[9] using K_2CO_3 in DMF afforded **19d**. The methyl ester of **19d** was hydrolyzed by 1M NaOH in MeOH to yield **19**.

3. Biology

The binding activity of the analogs to LBD of FXR was evaluated by TR-FRET-based coactivator recruitment assay.[13] Evaluation of FXR agonist activity and ligand activity for other nuclear receptors and TGR5 by these compounds in living cells was carried out by a luciferase assay as previously published.[50] Analysis of ligand-induced

regulation of FXR target genes was conducted using real time RT-PCR according to a previous report.[50] Values of *P* used to compare the statistical significance were determined using Student's t-test in Excel. Validation of activating differentiation of ST-2 MSCs into osteoblasts was conducted according to the literature.[13] Statistical analysis was performed using One-way ANOVA, followed by Tukey's *post hoc* test (Statcel 3 software; OMS Publishing, Saitama, Japan). The experimental protocols are available in Supplementary Data.

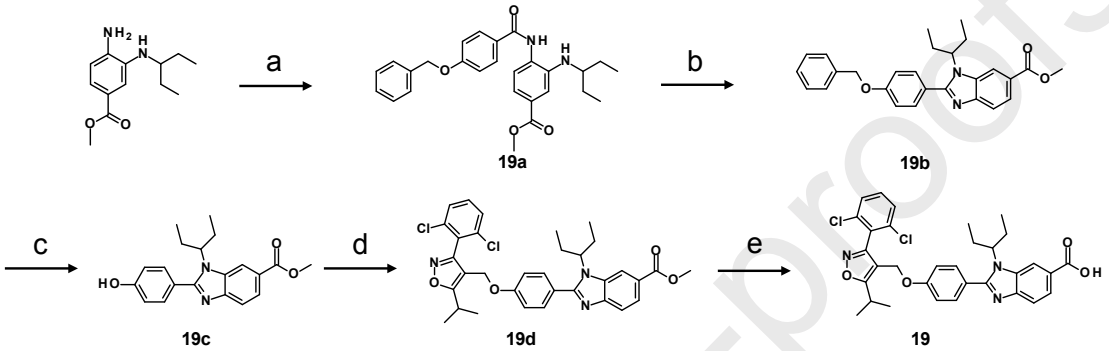

Scheme 1. Reagents and conditions: (a) 4-Benzyloxybenzoic acid, Et_3N, HOAt, WSCI.HCl, DMF, 15 h, 0 °C→ rt; (b) CH_3COOH, 2 h, 80 °C; (c) 10 % Pd/C, H_2, MeOH/THF, 15 h, rt; (d) 4-(Bromomethyl)-3-(2,6-dichlorophenyl)-5-isopropyl-isoxazole, K_2CO_3, DMF, 15 h, rt; (e) 1M NaOH, MeOH/THF, 15 h, rt.

4. Results and Discussion

Our efforts for the development of potent and selective FXR agonists began with a SAR exploration starting with the replacement of the N^1-methyl group on benzimidazole of **12**. The synthesized analogs (**16-39**) were assessed by an FXR time-resolved fluorescence resonance energy transfer (TR-FRET) binding assay and a luciferase reporter assay according to a previous publication.[13] An antagonistic activity against VDR as off-target was simultaneously evaluated, and the target selectivity was calculated from EC_{50} and IC_{50} measured by a luciferase assay and shown as the ratio of IC_{50} (VDR) / EC_{50} (FXR). The modification on the nitrogen atom in benzimidazole made a difference in the agonistic activity for FXR.

Replacing N^1-methyl group of **12** with various size substituents was carried out. (Table 2) The methyl moiety of **12** was replaced by linear alkyl groups, ethyl (**16**) and propyl (**17**). The former appeared to bind nearly 2- and 15-fold greater than **12** in TR-FRET binding and luciferase assays, respectively, and the inhibition against VDR was equivalent to that of **12**, resulting that a ratio of IC_{50} (VDR) / EC_{50} (FXR) exceeded 2000 times. Although the latter modification was inferior to **16** in either assay for FXR, it showed a single-digit nanomolar activity against FXR in the luciferase assay and a slight increase in the affinity toward VDR. In addition to the size (length) effect as seen

Table 2. Effects of **16**-**33** on FXR and VDR

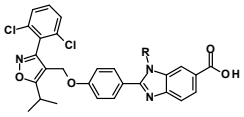

Cpds.	R	FXR EC_{50} (nM) TR-FRET	Relative potency (%)	FXR EC_{50} (nM) Luciferase	Relative potency (%)	VDR IC_{50} (nM) Luciferase	Relative potency (%)	VDR (IC_{50}) / FXR (EC_{50}) Luciferase
12*	CH_3	43.7±54.2	58.2±26.2	32.0±38.1	101.0±31.1	7151.3±3853.3	55.2±4.5	223
16		19.3±9.8	61.2±14.2	2.31±1.82	76.4±7.8	5760.9±748.3	66.0±8.6	2439
17		96.4±60.4	14.5±12.4	9.3±0.7	50.9±9.2	1401.3±290.2	86.2±1.5	150
18		56.7±63.6	27.6±20.2	3.39±1.61	56.3±3.7	3551.9±459.4	85.8±4.2	1047
19		26.5±10.5	68.7±10.9	0.8±0.2	70.4±2.5	5688.0±1431.8	51.7±0.7	7110
20		30.3±10.8	70.1±10.8	1.8±1.2	68.9±7.4	>10000	20.1±12.5	-
21		116.8±84.4	26.4±13.9	16.5±0.3	59.1±5.2	3197.7±714.1	78.1±2.0	193
22		-	-	14.4±1.5	50.8±3.9	1104.0±179.5	89.3±1.9	76
23		-	-	13.6±0.8	36.8±8.7	928.8±95.7	83.1±1.1	68
24		-	-	4.21±0.54	61.1±9.4	1448.6±201.3	68.9±5.4	344
25		113.4±93.0	31.0±9.1	14.8±2.4	55.6±6.9	921.1±55.3	76.8±2.9	62
26		-	-	1432.0±1672.3	3.9±3.1	>10000	0	-
27		24.7±14.0	23.5±11.2	5.26±4.58	66.6±7.42	1183.4±828.3	82.1±8.6	224
28		24.8±22.7	20.1±11.9	13.0±5.2	55.0±11.7	861.3±21.8	86.0±4.2	66
29		29.1±22.9	26.5±7.5	19.4±13.7	61.4±17.0	2652.5±1520.1	74.9±1.8	136
30		19.9±10.7	51.4±10.5	0.52±0.14	70.9±0.5	346.0±144.9	82.7±4.9	665
31		-	-	1166.1±1144.3	11.1±7.4	>10000	24.3±20.9	-
32		15.1±11.4	9.1±10.0	32.2±18.6	90.2±7.85	2413.8±2160.3	76.1±7.7	74
33		105.3±135.2	30.2±31.6	3.31±0.63	70.9±6.9	1141.6±430.3	76.2±3.4	344

-: Not determined

in **16** and **17**, we successively investigated the size (balkiness) of N^1-α-branched alkyl groups (**18-20**). The isopropyl group (**18**) had almost the same activity against FXR as the ethyl substituent (**16**) and a slight increase in the inhibitory activity against VDR, with a decrease in the selectivity ratio. The linear extension by branching (**19**) indicated that the agonistic activity against FXR was at and below nanomolar level (EC_{50} = 26.5 ± 10.5 nM TR-FRET, 0.8 ± 0.2 nM luciferase, respectively). Although **19** still retained weak antagonism against VDR (IC_{50} = 5688.0 ± 1431.8 nM), the ratio of IC_{50} (VDR) / EC_{50} (FXR) was more than 7000-fold. Further extension (**20**) of **19** showed a slight attenuation of the agonistic effect on FXR and complete loss of the antagonism against VDR relative to **19**. Since the N^1-α-branched analogs shared promising results in both assays for FXR, cyclic (**21-26**) and N^1-β-branched (**27-31**) analogs were evaluated.

Analogs **21-26** bearing cyclic substituents on benzimidazole revealed less activity than **19** in the luciferase assay for FXR but had a slight increase in the affinity with VDR compared to **19**. The selective ratios of **21-25** were, therefore, reduced as compared to **19**. An acylated piperidine moiety (**26**) showed no significant effect on FXR. N^1-β-Branched derivatives (**27** and **28**) preserved the agonistic activity against FXR in the luciferase assay at almost the same level as **21-25** and had an upward trend in the inhibitory activity against VDR. Extension of the chain length of the cyclopropyl ring showed no significant difference in the activity in the luciferase receptor assay (**21** vs **29**). Notably, robust potency was observed for **30** (EC_{50} = 19.9 ± 10.7 nM TR-FRET, 0.52 ± 0.14 nM luciferase), being nearly equipotent with **19**; besides, the substituent of **30** (IC_{50}=346.0±144.9 nM) facilitated the interaction with VDR. Like analog **26**, the substituent of **31** was not tolerated in either receptor. The aromatic substituents (**32** and **33**) were less favorable in the ratio of IC_{50} (VDR) / EC_{50} (FXR). It turns out that N^1-substituents of **19** and **20** represent key building blocks to achieve nanomolar level potency against on-target and lead to the selectivity ratio of IC_{50} (VDR) / EC_{50} (FXR) greater than 5000-fold.

We next attempted to determine whether the analogs (**34-37**) derived from **19** and **30** substantially cause the changes in agonism against FXR (Table 3) since **15** substantially changed it in the luciferase assay (**12** vs **15**).[13] Even if fluoride (**34**, **36**) and chloride (**35**, **37**) were introduced into **19** and **30**, respectively, there were no substantial changes in agonism (**34**, **35**) and the EC_{50} values in the luciferase assay of **36** and **37** increased about 10-fold compared to that of **30**. Introduction of fluoride (**34**, **36**) and chloride (**35**, **37**) revealed a counter trend on the antagonism against VDR relative to **19** and **30**, respectively. This observation led to the discovery of **34**, which exhibited an EC_{50} = 69.9 ± 22.0 nM in TR-FRET and EC_{50} = 1.3 ± 0.2 nM in the luciferase assay and loss of antagonism against VDR.

Table 3. Effects of **34**-**37** on FXR and VDR

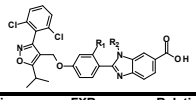

Cpds.	R_1	R_2	FXR EC_{50} (nM) TR-FRET	Relative potency (%)	FXR EC_{50} (nM) Luciferase	Relative potency (%)	VDR IC_{50} (nM) Luciferase	Relative potency (%)	VDR(IC_{50})/ FXR(EC_{50}) Luciferase
19	H		26.5±10.5	68.7±10.9	0.8±0.2	70.4±2.5	5688.0±1431.8	51.7±0.7	7110
34	F		69.3±22.0	48.7±12.9	1.3±0.2	43.1±6.9	>10000	54.7±11.5	-
35	Cl		21.6±12.7	95.8±12.9	1.6±0.03	54.5±11.7	1012.6±43.9	74.0±2.8	632
30	H		19.9±10.7	51.4±10.5	0.52±0.14	70.9±0.5	346.0±144.9	82.7±4.9	665
36	F		-	-	7.8±2.9	58.0±6.5	839.5±86.9	78.8±3.0	49
37	Cl		66.1±53.8	18.7±5.5	7.6±1.9	53.9±8.8	160.3±8.9	76.5±5.9	21

-: Not determined

Our computer-assisted modeling studies suggested that **19** (white) and **30** (white) (left and right panels in Figure 2, respectively) occupy the same binding site of LBD in FXR as GW4064 (yellow) and exhibit interactions between the acidic moieties of each agonist and Arg331. (Figure 2) The N^1-α-branched alkyl group of **19** and N^1-α-branched cyclohexyl group of **30** are similarly placed in the vacant space of LBD that GW4064 does not fill. Both groups are hydrophobic and therefore may contribute to enhancing the EC_{50} activities for FXR because the cholesterol binding-site of FXR-LBD is known to be hydrophobic in nature.[51]

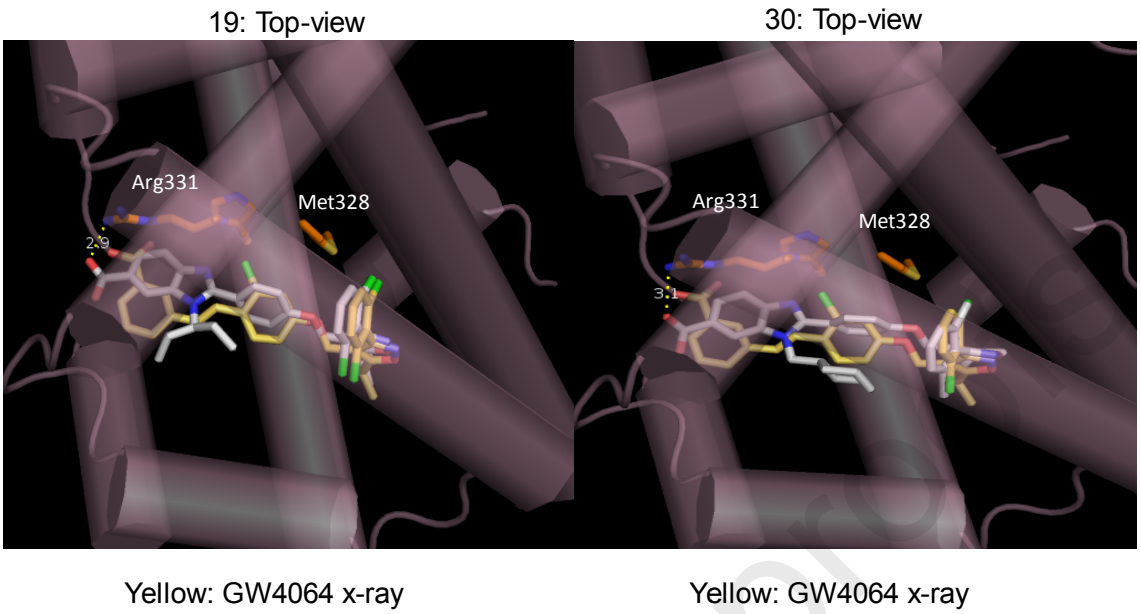

Figure 2. Modeling of FXR complexed with GW4064, **19** and **30**.
A complex-model of human FXRα-LBD monomer (PDB ID: 3DCT, purple cylinders and orange sticks) with GW4064 (X-ray; yellow sticks) and **19** (left panel, white sticks) and **30** (right panel, white sticks) was built using AutoDock Vina1.1.2.

The acidic moiety of our chemotype interacts with Arg331 in FXR through a hydrogen bond. (Figure 2) Contribution of this moiety relative to FXR activity was confirmed by **38** and **39**, which lack acidic moiety of **30**. (Table S1) The affinity with FXR and VDR of both analogs dropped sharply. The results revealed that the acidic moiety on N^1-substituted benzimidazole is required for the interaction with LBD in FXR.

Tetrazolium colorimetric (MTT) assays are the most common employed for the detection of cytotoxicity or cell viability following exposure to toxic substances.[52] As Huh-7 and HEK293T cells were used for the assay of agonism toward FXR and antagonism against VDR, respectively, the cytotoxic activities of the synthesized analogs in both cell lines were evaluated (Table S2). The results obtained in the MTT assays suggested that cytotoxicity tends to be partially affected by altering N^1-substituents on benzimidazole.

To gain insights into the agonism and target engagement for **19** (Figure 3) and **20** (Figure S1), the effect in modulating FXR target genes, BSEP, SHP and OSTα, was assessed in a Huh-7 cell line by real-time PCR, with GW4064 (0.01-1 μM) as the reference compound. Analogs **19** and **20** at 0.01-1 μM concentrations were as potent as GW4064 in the induction of mRNA expression.

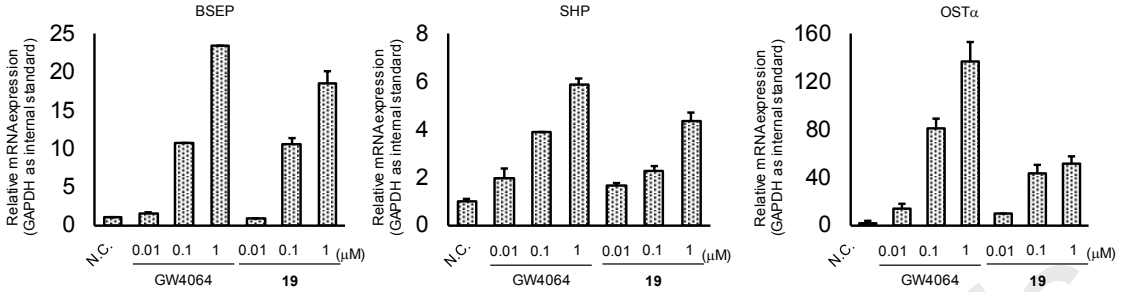

Figure 3. Effect of **19** on FXR target genes. Expression of FXR-induced genes BSEP, SHP and OSTα was significantly increased by treatment of GW4064 or **19** in Huh-7 cells (n=3, $P < 0.01$ v.s. N.C.)

Further, *in vitro* profile of **19** and **20** was expanded to common off-targets for bile acid receptor ligands. (Figure 4 and Figure S2, respectively) Both analogs were unable to induce RXRα, RARα, VDR, PPARα, γ and δ, LXRα and β, TGR5 transactivation on Huh-7 cell lines. In brief, both analogues **19** and **20** (1 μM) had no agonism toward any of these receptors other than FXR.

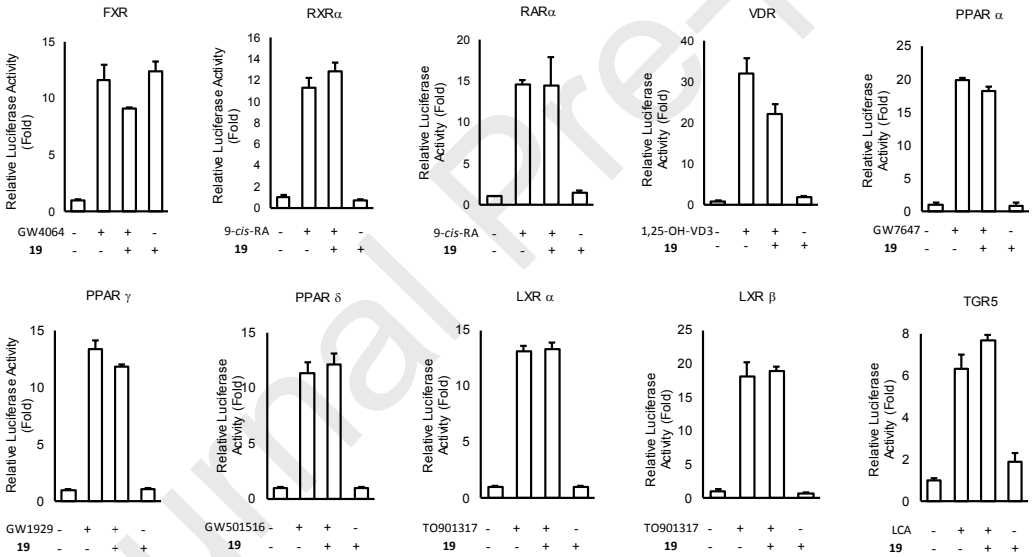

Figure 4 .Selectivity screening of **19** against human nuclear receptors and TGR5. The concentration of ligands for each nuclear receptor was as follows; **19**: 1 μM, GW4064: 100 nM, 9-*cis*-retinoic acid (9-*cis*-RA): 50 nM, 1,25-hydroxyvitamin D_3 (1,25-OH-VD_3): 100nM, Lithocholic acid (LCA): 200nM, GW7647: 50nM, GW501516: 50nM, GW1929: 50nM, TO901317: 50nM.

We subsequently investigated whether **19** and **30** activate the BMP-2-induced differentiation of ST-2 MSCs into osteoblasts, like **14** and **15** according to a previous publication.[13] At first, viability of ST-2 MSCs in the presence of **19** or **30** was evaluated by a WST-8 assay (Figure 5A) Cells were cultured for 12 days in RPMI-1640 medium containing various concentrations of **19** or **30** (0−10 μM); no significant toxic effects were observed up to 5 μM in the cells. The ST-2 MSCs differentiated into osteoblasts after 6 or 12 days in RPMI-1640 medium with BMP-2 in the presence or absence of

FXR agonists. The staining and activity of alkaline phosphatase (ALP) that is the biomarker of bone formation[53] were enhanced by treatment with BMP-2 during osteoblast differentiation of ST-2 MCSs after 6 days and 12 days. (Figure 5B, C) Enhancing the staining and activity of ALP was clearly observed for FXR agonists including **19** and **30** and the activity was repressed by the co-treatment with guggulsterone (GS).[54] (Figure 5B, C) Thus, our structure-activity analyses of N^1-substituents on benzimidazole culminated in the identification of a remarkable series of FXR agonists bearing potency below nanomolar level.

5. Conclusion

We have developed a series of FXR agonists with different N^1-substituents on the benzimidazole pharmacophore as potential modulators of FXR. As exemplified by **19** and **30**, the size (length and bulkiness) of N^1-substituents greatly affected antagonism against FXR as on-target and the selective ratio of on-target versus off-target. Unfortunately, no clear SAR on the analogs reported here against FXR and VDR was apparent, but **19**, **20** and **34**, which share N^1-α-branched aliphatic group, led to an increase in potency for FXR and nearly a complete loss of antagonism against VDR. Analog **19** was an FXR agonist: the affinity with FXR over eight nuclear receptors and TGR-5, effects on FXR target genes, and ALP activity BMP-2-induced differentiation of ST-2 MSCs into osteoblast. Furthermore, molecular modeling implied that **19** fills the leeway of LBD in FXR that the stilbene of GW4064 (**1**) cannot cover, resulting that **19** shares agonism against FXR below nanomolar level. In contrast, introduction of slightly bulkier cyclic group than that of **19**, as observed with **30**, facilitated the interaction with VDR and increased the potency for VDR even though **30** showed the similar agonism against FXR as **19**. According to selective optimization of side activities (SOSA) concept,[55] the chemical modification of **30** may serve to develop the new chemotype for future non-secosteroidal VDR ligands as the modification of omeprazole led to the discovery of nanomolar bombesin receptor subtype 3 agonists.[56]

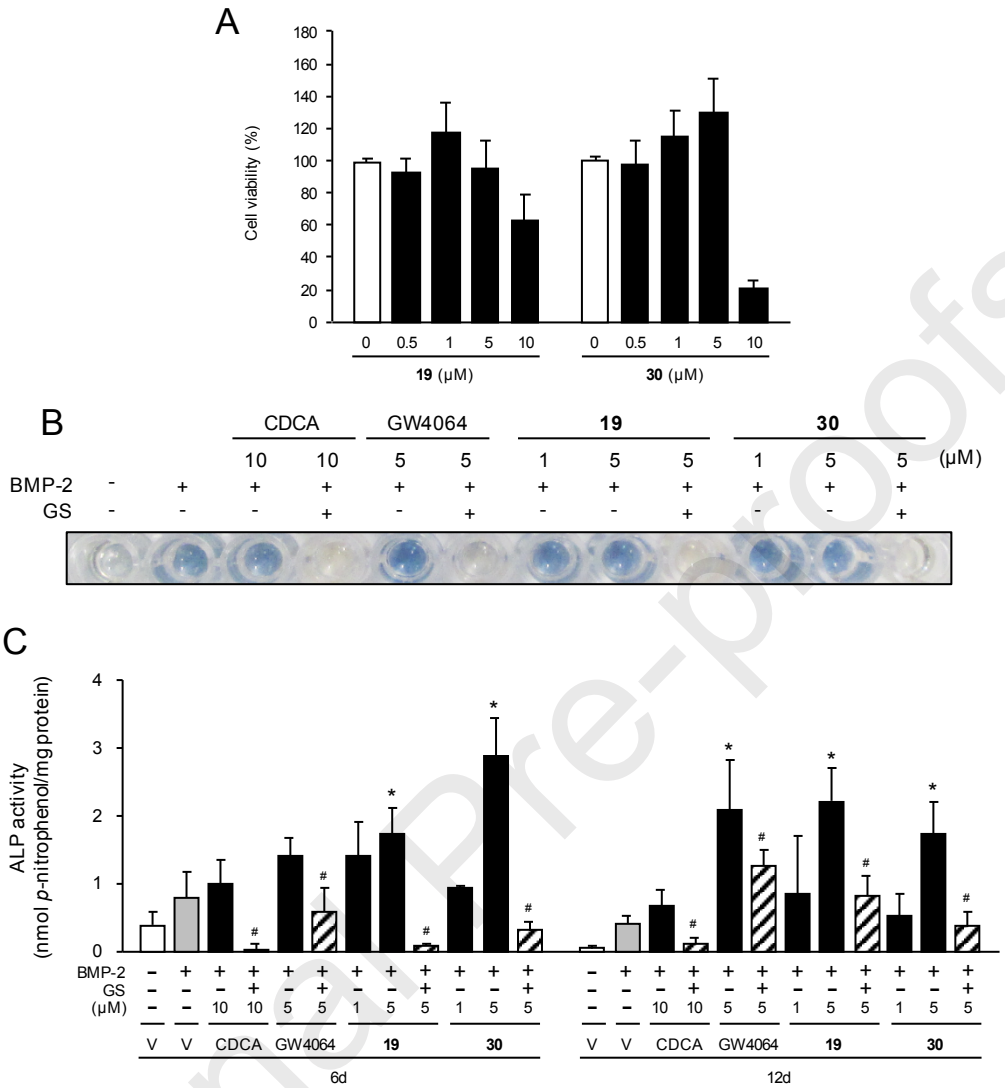

Figure 5. Activation of BMP-2-induced osteoblast differentiation by novel synthesized FXR agonist **19** and **30** in ST-2 MSCs. (A) Cell viability. The ST-2 MSCs (vehicle; white columns) were cultured for 12 days in the medium containing 0-10 μM of **19** or **30** (black columns). Cell viability was measured by a WST-8 assay. Cell viability at 0 μM was defined as 100%. Data are presented as means ± S.D.(n=5). (B) ALP staining. The ST-2 MSCs were differentiated into osteoblasts for 12 days in the medium containing BMP-2 (50 ng/ml) together with 10 μM CDCA, 5 μM GW4064, or 1 or 5 μM of **19** or **30** in the presence or absence of 25 μM GS. ALP staining was performed as described in Materials and Methods. The results are the representative from three experiments. (C) ALP activity. The ST-2 MSCs (vehicle: V; white columns) were cultured for 6 or 12 days in the medium containing BMP-2 (50 ng/ml; gray columns) together with one of the FXR agonists, 10 μM CDCA, 5 μM GW4064, and 1 or 5 μM of **19** or **30** (black columns) in the presence or absence of 25 μM GS (hatched columns). Data are shown as means ± S.D.(n=3). *p<0.01, as compared with the BMP-2-induced cells, #p<0.01, as compared with the FXR agonist-treated cells.

6. Experimentals

6.1 Materials and Methods

All chemicals were purchased from Tokyo Chemical Industry Co., Ltd., FUJIFILIM Wako Pure Chemical Industries, Ltd. or Aurora Fine Chemicals LLC and used without further purification. All protected amino acids and the coupling reagents were purchased from Watanabe Chemical Industries, Ltd. ^{1}H-NMR experiments were recorded on a

JMTC-600 (JEOL Ltd.) 600 NMR spectrometer with $CDCl_3$ or DMSO-d_6 as solvents. Chemical shifts are expressed in parts per million (ppm, δ) and referred to the solvent signal. HRMS spectra were recorded on The AccuTOF (JMS-T100LC) equipped with an electrospray ion source (JEOL Ltd.). The analytical HPLC system consisted of a SHINADZU CBM-20A System Controller and a SHINADZU Pump Unit LC-20AT, a SHIMADZU In-Line Degasser DGU-$20A_{3R}$, a SHIMADZU SPD-20A Absorbance Detector, a SHIMADZU FCV-11AL Valve Unit and a SHIMADZU FRC-10A Fraction Collector (SHIMADZU Corporation). The absorbance detector was operated at 254 nm. The mobile phase for preparation and analysis was a combinations of water (A) and acetonitrile (B), both containing 0.1% TFA, and a flow rate of 1 ml/min, respectively. TSK gel ODS column (4.6 x 150 mm for analysis, TOSOH Corporation) were used.

6.2. Methyl 4-[(4-benzyloxybenzoyl)amino]-3-(1-ethylpropylamino)benzoate (19a) : Methyl 4-amino-3-(1-ethylpropylamino)benzoate[50] (172 mg, 0.73 mmol) in DMF (5 ml) was added to a solution of 4-benzyloxybenzoic acid (166 mg, 0.73 mmol) in DMF (2 ml) at 0 °C. Subsequently, HOAt (119 mg, 0.88 mmol), WSCI.HCl (207 mg, 1.09 mmol) and Et_3N (306 µl, 2.19 mmol) were added to the former solution at 0 °C and stirred for 15 h at room temperature. The reaction mixture was quenched with sat.$NaHCO_3$ and extracted with EtOAc. The combined extracts were washed with H_2O and brine, dried over $MgSO_4$ and concentrated under reduced pressure. The residue was purified by silica gel column chromatography to give **19a** in 61 % yield. Rf=0.48 (*n*-Hexane/EtOAc=2/1). ^{1}H NMR (600 MHz, $CDCl_3$): δ 8.11 (brs, 1H), 7.87 (d, J=8.5 Hz, 2H), 7.77 (brs, 1H), 7.56-7.54 (m, 2H), 7.44-7.34 (m, 5H), 7.07 (d, J=8.8 Hz, 2H), 5.15 (s, 2H), 3.91 (s, 3H), 3.40 (brs, 1H), 3.24-3.22 (m, 1H), 1.63-1.48 (m, 4H), 0.94 (t, J=7.5 Hz, 6H). HRMS (ESI/TOF) m/z: $[M+H]^+$ Calcd for $C_{27}H_{31}N_2O_4$ 447.22838 ; Found 447.22575.

6.3. Methyl 2-(4-benzyloxyphenyl)-3-(1-ethylpropyl)benzimidazole-5-carboxylate (19b) : 19a (197 mg, 0.44 mmol) was dissolved in CH_3COOH (5 ml) at room temperature and stirred for 2 h at 80 °C. The reaction mixture was evaporated and quenched by addition of sat.$NaHCO_3$. The mixture was extracted with EtOAc, and organic layer was washed successively with H_2O and brine, dried over $MgSO_4$ and concentrated under reduced pressure. The residue was purified by silica gel column chromatography to give **19b** in 86 % yield. Rf=0.28 (*n*-Hexane/EtOAc=2/1). ^{1}H NMR (600 MHz, $CDCl_3$): δ 8.30 (s, 1H), 8.00 (d, J=8.4 Hz, 1H), 7.81 (d, J=8.5 Hz, 1H), 7.56 (d, J=7.8 Hz, 2H), 7.47 (d, J=7.7 Hz, 2H), 7.42 (t, J=7.6 Hz, 2H), 7.36 (t, J=6.8 Hz, 1H),

7.12 (d, J=8.7 Hz, 2H), 5.15 (s, 2H), 4.30-4.26 (m, 1H), 3.97 (s, 3H), 2.23-2.20 (m, 2H), 2.00-1.96 (m, 2H), 0.74 (t, J=7.3, 6H). HRMS (ESI/TOF) m/z: $[M+H]^+$ Calcd for $C_{27}H_{29}N_2O_3$ 429.21782 ; Found 429.21805.

6.4. Methyl 3-(1-ethylpropyl)-2-(4-hydroxyphenyl)benzimidazole-5-carboxylate (19c) : To **19b** (161 mg, 0.38 mmol) and 10 % Pd/C (40 mg), was added dist.MeOH/dist.THF (2.5 ml/2.5 ml) and hydrogenated under a hydrogen atmosphere for 15 h at room temperature. The solution was filtered and concentrated under reduced pressure to give **19c** in quantitative yield. Rf=0.59 (*n*-Hexane/EtOAc=1/2). ^{1}H NMR (600 MHz, $CDCl_3$): δ 9.76 (brs, 1H), 8.31 (s, 1H), 8.02 (dd, J=8.5, 1.5 Hz, 1H), 7.84 (d, J=8.5 Hz, 1H), 7.36 (d, J=8.6 Hz, 2H), 6.84 (d, J=8.6 Hz, 2H), 4.31-4.26 (m, 1H), 3.97 (s, 3H), 2.23-2.18 (m, 2H), 2.00-1.95 (m, 2H), 0.74 (t, J=7.4 Hz, 6H). HRMS (ESI/TOF) m/z: $[M+H]^+$ Calcd for $C_{20}H_{23}N_2O_3$ 339.17087 ; Found 339.17323.

6.5. Methyl 2-[4-[[3-(2,6-dichlorophenyl)-5-isopropyl-isoxazol-4-yl]methoxy]phenyl]-3-(1-ethyl propyl)benzimidazole-5-carboxylate (19d) : To a solution of **19c** (70 mg, 0.21 mmol) and 4-(bromomethyl)-3-(2,6-dichlorophenyl)-5-isopropyl-isoxazole[30] (72 mg, 0.21 mmol) in DMF (4 ml), K_2CO_3 (57 mg, 0.41 mmol) was added at room temperature and stirred for 15 h at room temperature. The reaction mixture was quenched with sat.NH_4Cl and extracted with EtOAc. The combined extracts were washed with H_2O and brine, dried over $MgSO_4$ and concentrated under reduced pressure. The residue was purified by silica gel column chromatography to give **19d** in 95 % yield. Rf=0.65 (*n*-Hexane/EtOAc=1/1). ^{1}H NMR (600 MHz, $CDCl_3$): δ 8.29 (s, 1H), 7.99 (d, J=8.5 Hz, 1H), 7.79 (d, J=8.5 Hz, 1H), 7.49 (d, J=8.1 Hz, 2H), 7.41 (d, J=8.2 Hz, 2H), 7.34 (t, J=8.8 Hz, 1H), 6.90 (d, J=8.2 Hz, 2H), 4.82 (s, 2H), 4.25-4.20 (m, 1H), 3.96 (s, 3H), 3.39-3.34 (m, 1H), 2.23-2.18 (m, 2H), 1.99-1.93 (m, 2H), 1.45 (d, J=7.0 Hz, 6H), 0.73-0.70 (m, 6H). HRMS (ESI/TOF) m/z: $[M+H]^+$ Calcd for $C_{33}H_{34}Cl_2N_3O_4$ 606.19264 ; Found 606.19148.

6.6. 2-[4-[[3-(2,6-Dichlorophenyl)-5-isopropyl-isoxazol-4-yl]methoxy]phenyl]-3-(1-ethylpropyl)benzimidazole-5-carboxylic acid (19) : To a suspension of **19d** (118 mg, 0.20 mmol) in MeOH/THF (2 ml/2 ml), 1M NaOH (0.98 ml, 0.98 mmol) was added at room temperature and the mixture was stirred for 15 h at room temperature. The reaction mixture was neutralized with 1M HCl and evaporated down. A white solid product appeared and filtered to give 96 mg of **19** in 51 % yield. Rf=0.63

(CH_2Cl_2/MeOH=9/1), ^{1}H NMR (600 MHz, DMSO-d_6): δ 13.2 (brs, 1H), 8.37 (s, 1H), 8.02 (d, J=8.3 Hz, 1H), 7.87 (d, J=8.4 Hz, 1H), 7.71 (d, J=8.1 Hz, 2H), 7.64-7.60 (m, 3H), 7.11 (d, J=8.5 Hz, 2H), 5.03 (s, 2H), 4.28 (m, 1H), 3.58-3.54 (m, 1H), 2.16-2.03 (m, 4H), 1.42 (d, J=7.0 Hz, 6H), 0.74-0.69 (m, 6H). ^{13}C NMR (600 MHz, DMSO-d_6): δ 175.7, 167.0, 159.2, 158.5, 155.6, 142.2, 134.3, 132.1, 131.6, 131.1, 128.1, 126.8, 125.3, 124.1, 120.1, 117.5, 114.7, 114.1, 108.9, 61.0, 58.7, 25.7, 25.6, 20.3, 10.4. HRMS (ESI/TOF) m/z: $[M+H]^+$ Calcd for $C_{32}H_{32}Cl_2N_3O_4$ 592.17699 ; Found 592.17973.

Acknowledgements

We are grateful to Dr. Lawrence H. Lazarus for critically reading the manuscript. We thank Professor Hidetoshi Tahara for data collection.

Supplementary data

Supplementary data associated with this article can be found, in the online version, at XXX.

References

[1] Zhang Z, Burch PE, Cooney AJ. Lanz RB, Pereira FA, Wu J, Gibbs RA, Weinstock G, Wheeler DA. Genomic analysis of the nuclear receptor family: new insights into structure, regulation, and evolution from the rat genome. *Genome Res.* 2004;14: 580-590. doi:10.1101/gr.2160004

[2] Makishima M, Okamoto AY, Repa JJ, Tu H, Learned RM, Luk A, Hull MV, Lustig KD, Mangelsdorf DJ, Shan B. Identification of a nuclear receptor for bile acids. *Science.* 1999;284:1362-1365. doi: 10.1126/science.284.5418.1362.

[3] Parks DJ, Blanchard SG, Bledsoe RK, Chandra G, Consler TG, Kliewer SA, Stimmel JB, Willson TM, Zavacki AM, Moore DD, Lehmann JM. Bile acids: Natural ligands for an orphan nuclear receptor. *Science.* 1999;284:1365-1368. doi: 10.1126/science.284.5418.1365.

[4] Handschin C, Meyer UA. Regulatory network of lipid-sensing nuclear receptors: roles for CAR, PXR, LXR, and FXR. *Arch Biochem Biophys.* 2005;433:387-396. doi: 10.1016/j.abb.2004.08.030

[5] Kakizaki S, Yamazaki Y, Takizawa D, Negishi M. New insights on the xenobiotic-sensing nuclear receptors in liver diseases -CAR and PXR- *Curr Drug Metabolism.* 2008;9:614-621. doi.org/10.2174/138920008785821666

[6] Chiang JYL. Bile acids: regulation of synthesis. *J Lipid Res*. 2009;50:1955-1966. doi: 10.1194/jlr.R900010-JLR200

[7] Inagaki T, Choi M, Moschetta A, Peng L, Cummins CL, McDonald JG, Luo G, Jones SA, Goodwin B, Richardson JA, Gerard RD, Repa JJ, Mangelsdorf DJ, Kliewe SA. Fibroblast growth factor 15 functions as an enterohepatic signal to regulate bile acid homeostasis. *Cell Metabolism*. 2005;2:217-225. doi: 10.1016/j.cmet.2005.09.001.

[8] Dawson PA, Lan T, Rao A. Bile acid transporters. *J Lipid Res*. 2009;50:2340-2357. doi: 10.1194/jlr.R900012-JLR200.

[9] Chou CC, Yang JS, Lu HF, Ip SW, Lo C, Wu CC, Lin JP, Tang NY, Chung JG, Chou MJ, Teng YH, Chen DR. Quercetin-mediated cell cycle arrest and apoptosis involving activation of a caspase cascade through the mitochondrial pathway in human breast cancer MCF-7 cells. *Arch Pharm Res*. 2010;33:1181-1191. doi.org/10.1007/s12272-010-0808-y

[10] Id Boufker H, Lagneaux L, Fayyad-Kazan H, Badran B, Najar M, Wiedig M, Ghanem G, Laurent G, Body JJ, Journe F. Role of farnesoid X receptor (FXR) in the process of differentiation of bone marrow stromal cells into osteoblasts. *Bone*. 2011;49: 1219-1231. doi.org/10.1016/j.bone.2011.08.013

[11] Cho SW, An JH, Park H, Yang JY, Choi HJ, Kim SW, Park YJ, Kim SY, Yim M, Baek WY, Kim JE, Shin CS. Positive regulation of osteogenesis by bile acid through FXR. *J Bone Miner Res.* 2013;28:2109-2121. doi.org/10.1002/jbmr.1961

[12] Jeong BC, Lee YS, Bae IH, Lee CH, Shin HI, Ha HJ, Franceschi RT, Choi HS, Koh JT. The orphan nuclear receptor SHP is a positive regulator of osteoblastic bone formation. *J Bone Miner Res*. 2010;25:262-274. doi.org/10.1359/jbmr.090718

[13] Fujimori K, Iguchi Y, Yamashita Y, Gohda K, Teno N. Synthesis of novel farnesoid X receptor agonists and validation of their efficacy in activating differentiation of mouse bone marrow-derived mesenchymal stem cells into osteoblasts. *Molecules*. 2019;24:4155. doi: 10.3390/molecules24224155

[14] Tully DC, Rucker PV, Chianelli D, Williams J, Vidal A, Alper PB, Mutnick D, Bursulaya B, Schmeits J, Wu X, Bao D, Zoll J, Kim Y, Groessl T, McNamara P, Seidel HM, Molteni V, Liu B, Phimister A, Joseph SB, Laffitte B. Discovery of tropifexor (LJN452), a highly potent non-bile acid FXR agonist for the treatment of cholestatic liver diseases and nonalco-holic steatohepatitis (NASH). *J Med Chem.* 2017;60:9960−9973. doi.org/10.1021/acs.jmedchem.7b00907

[15] Akwabi-Ameyaw A, Bass JY, Caldwell RD, Caravella JA, Chen L, Creech KL, Deaton DN, Jones SA, Kaldor I, Liu Y, Madauss KP, Marr HB, McFadyen RB, Miller AB, Navas III F, Parks DJ, Spearing PK, Todd D, Williams SP, Wisely GB. Conformationally constrained farnesoid X receptor (FXR) agonists: Naphthoic acid-based analogs of GW 4064. *Bioorg Med Chem Lett.* 2008;18:4339-4343. doi:10.1016/j.bmcl.2008.06.073.

[16] Bass JY, Caldwell RD, Caravella JA, Chen L, Creech KL, Deaton DN, Madauss KP, Marr HB, McFadyen RB, Miller AB, Parks DJ, Todd D, Williams SP, Wisely GB. Substituted isoxazole analogs of farnesoid X receptor (FXR) agonist GW4064. *Bioorg Med Chem Lett*. 2009;19:2969-2973. doi:10.1016/j.bmcl.2009.04.047.

[17] Akwabi-Ameyaw A, Bass JY, Caldwell RD, Caravella JA, Chen L, Creech KL, Deaton DN, Madauss KP, Marr HB, McFadyen RB, Miller AB, Navas III F, Parks DJ, Spearing PK, Todd D, Williams SP, Wisely GB. FXR agonist activity of conformationally constrained analogs of GW 4064. *Bioorg Med Chem Lett*. 2009;19: 4733-4739. doi:10.1016/j.bmcl.2009.06.062.

[18] Bass JY, Caravella JA, Chen L, Creech KL, Deaton DN, Madauss KP, Marr HB, McFadyen RB, Miller AB, Mills WY, Navas III F, Parks DJ, Smalley Jr TL, Spearing PK, Todd D, Williams SP, Wisely GB. Conformationally constrained farnesoid X receptor (FXR) agonists: heteroaryl replacements of the naphthalene. *Bioorg Med Chem Lett.* 2011;21:1206-1213. doi:10.1016/j.bmcl.2010.12.089.

[19] Akwabi-Ameyaw A, Caravella JA, Chen L, Creech KL, Deaton DN, Madauss KP, Marr HB, Miller AB, Navas III F, Parks DJ, Spearing PK. Todd D, Williams SP, Wisely GB. Conformationally constrained farnesoid X receptor (FXR) agonists: Alternative replacements of the stilbene. *Bioorg Med Chem Lett*, 2011;21:6154-6160. doi:10.1016/j.bmcl.2011.08.034.

[20] Smalley Jr TL, Boggs S, Caravella JA, Chen L, Creech KL, Deaton DN, Kaldor I, Parks DJ. Novel heterocyclic scaffolds of GW4064 as farnesoid X receptor agonists. *Bioorg Med Chem Lett*. 2015;25:280-284. doi:10.1016/j.bmcl.2014.11.050.

[21] Genin MJ, Bueno AB, Francisco JA, Manninen PR, Bocchinfuso WP, Montrose-Rafizadeh C, Cannady EA, Jones TM, Stille JR, Raddad E, Reidy C, Cox A, Michael MD, Michael LF. Discovery of 6-(4-{[5-Cyclopropyl-3-(2,6-dichlorophenyl)isoxazol-4-yl]methoxy}piperidin-1-yl)-1-methyl-1H-indole-3-carboxylic acid: A novel FXR agonist for the treatment of dyslipidemia. *J Med Chem.* 2015;58:9768-9772. doi:10.1021/acs.jmedchem.5b01161.

[22] Kinzel O, Steeneck C, Schlüter T, Schulz A, Gege C, Hahn U, Hambruch E, Hornberger M, Spalwisz A, Frick K, Perovic´-Ottstadt S, Deuschle U, Burnet M, Kremoser C. Novel substituted isoxazole FXR agonists with cyclopropyl, hydroxycyclobutyl and hydroxyazetidinyl linkers: Understanding and improving key determinants of pharmacological properties. *Bioorg Med Chem Lett.* 2016;26:3746-3753. doi:10.1016/j.bmcl.2016.05.070.

[23] Sepe V, Marchianò S, Finamore C, Baronissi G, Di Leva FS, Carino A, Biagioli M, Fiorucci C, Cassiano C, Monti MC, del Gaudio F, Novellino E, Limongelli V, Fiorucci S, Zampella A. Novel isoxazole derivatives with potent FXR agonistic activity prevent acetaminophen-induced liver injury. *ACS Med Chem Lett.* 2019;10:407-412. doi:10.1021/acsmedchemlett.8b00423.

[24] Deaton DN, Navas FI, Spearing PK. Farnesoid X receptor agonists. WO2008152270, 2008.

[25] Hosoda S, Hashimoto Y. Structural development studies of nuclear receptor ligands. *Pure Appl Chem.* 2007;79:615-626. doi: 10.1351/pac200779040615

[26] Flesch D, Gabler M, Lill A, Gomez RC, Steri R, Schneider G, Stark H, Schubert-Zsilavecz M, Merk D. Fragmentation of GW4064 led to a highly potent partial farnesoid X receptor agonist with improved drug-like properties. *Bioorg Med Chem.* 2015;23:3490-3498, doi:10.1016/j.bmc.2015.04.035.

[27] Merk D, Lamers C, Ahmad K, Carrasco GR, Schneider G, Steinhilber D, Schubert-Zsilavecz M. Extending the structure-activity relationship of anthranilic acid derivatives as farnesoid X receptor modulators: development of a highly potent partial

farnesoid X receptor agonist. *J Med Chem.* 2014;57:8035-8055. doi:10.1021/jm500937v.

[28] Flesch D, Cheung SY, Schmidt J, Gabler M, Heitel P, Kramer J, Kaiser A, Hartmann M, Lindner M, Lüddens-Dämgen K, Heering J, Lamers C, Lüddens H, Wurglics M, Proschak E, Schubert-Zsilavecz M, Merk D. Nonacidic farnesoid X receptor modulators. *J Med Chem*. 2017;60:7199-7205. doi:10.1021/acs.jmedchem.7b00903.

[29] Wang H, Zhao Z, Zhou J, Guo Y, Wang G, Hao H, Xu X. A novel intestinal-restricted FXR agonist. *Bioorg Med Chem Lett.* 2017;27:3386-3390, doi:10.1016/j.bmcl.2017.06.003.

[30] Maloney PR, Parks DJ, Haffner CD, Fivush AM, Chandra G, Plunket KD, Creech KL, Moore LB, Wilson JG, Lewis MC, Jones SA, Willson TM. Identification of a chemical tool for the orphan nuclear receptor FXR. *J Med Chem*. 2000;43:2971-2974. doi.org/10.1021/jm0002127.

[31] Yu DD, Lin W, Chen T, Forman BM. Development of time resolved fluorescence resonance energy transfer-based assay for FXR antagonist discovery. *Bioorg Med Chem.* 2013;21:4266-4278. doi: 10.1016/j.bmc.2013.04.069

[32] Richter HGF, Benson GM, Bleicher KH, Blum D, Chaput E, Clemann N, Feng S, Gardes C, Grether U, Hartman P, Kuhn B, Martin RE, Plancher JM, Rudolph MG, Sculer F, Taylor S. Optimization of a class of benzimidazole-based farnesoid X receptor (FXR) agonists to improve physicochemical and ADME properties. *Bioorg Med Chem Lett*. 2011;21:1134-1140. doi:10.1016/j.bmcl.2010.12.123.

[33] Sanoh S, Kitamura S, Sugihara K, Fujimoto N, Ohta S. Estrogenic activity of stilbene derivatives. *J Health Sci*. 2003;49:359-367. doi: 10.1248/jhs.49.359

[34] Sanoh S, Kitamura S, Sugihara K, Kohta R, Ohta S, Watanabe H. Effects of stilbene and related compounds on reproductive organs in B6C3F1/Crj mouse. *J Health Sci*. 2006;52:613-622. doi: 10.1248/jhs.52.613

[35] Seidegård J, DePierre JW, Morgenstern R, Pilotti Å, Ernster L. Induction of durg-metabolizing systems and related enzymes with metabolites and structural analogues of stilbene. *Biochim Biophys Acta*. 1981;672:65-78. doi: 10.1016/0304-4165(81)90280-4

[36] Kuo CH, Hook JB, Bernstein J. Induction of drug-metabolizing enzymes and toxicity of *trans*-stilbene oxide in rat liver and kidney. *Toxicology*. 1981;22:149-160. doi: 10.1016/0300-483X(81)90114-1

[37] Sugihara K, Kitamura S, Sanoh S, Ohta S, Fujimoto N, Maruyama S, Ito A. Metabolic activation of the proestrogens *trans*-stilbene and *trans*-stilbene oxide by rat

liver microsomes. *Toxicol Appl Pharmacol.* 2000;167:46-54. doi: 10.1006/taap.2000.8979

[38] Romero FA, Jones C, Xu Y, Fenaux M, Halcomb RL. The race to bash NASH: Emerging targets and drug development in a complex liver disease. *J Med Chem.* 2020, *in press.* doi.org/10.1021/acs.jmedchem.9b01701

[39] Terns Pharmaceuticals: TERN-101. https://www.ternspharma.com/6-13-19-terns-pharmaceuticals-initiates-a-phase-1-clinical-trial-of-tern-101 (September 25, 2019).

[40] Kinzel O, Steeneck C, Kremoser C. Novel FXR (NR1H4) binding and activity modulating compounds. WO2013007387, 2013.

[41] Krasowski MD, Ni A, Hagey LR. Ekins S. Evolution of promiscuous nuclear hormone receptors: LXR, FXR, VDR, PXR, and CAR. *Mol Cell Endocrinol.* 2011;334: 39-48. doi:10.1016/j.mce.2010.06.016.

[42] Dusso AS, Brown AJ, Slatopolsky E. Vitamin D. *Am J Physiol Renal Physiol.* 2005;289:F8-F28. doi:10.1152/ajprenal.00336.2004.

[43] Reschly EJ, Ai N, Ekins S, Welsh WJ, Hagey LR, Hofmann AF, Krasowski MD. Evolution of the bile salt nuclear receptor FXR in vertebrates. *J Lipid Res.* 2008;49: 1577-1587. doi: 10.1194/jlr.M800138-JLR200.

[44] Maestro MA, Molnár F, Carlberg C. Vitamin D and its synthetic analogs. *J Med Chem.* 2019;62:6854-6875. doi: 10.1021/acs.jmedchem.9b00208

[45] Maruyama K, Noguchi-Yachide T, Sugita K, Hashimoto Y, Ishikawa M. Novel selective anti-androgens with a diphenylpentane skeleton. *Bioorg Med Chem Lett.*, 2010:20:6661-6666. doi: 10.1016/j.bmcl.2010.09.011

[46] Khedkar SA, Samad MA, Choudhury S, Lee JY, Zhang D, Thadhani RI, Karumanchi SA, Rigby AC, Kang PM. Identification of novel nonsecosteroidal vitamin D receptor agonists with potent cardioprotective effects and devoid of hypercalcemia. *Sci Rep.* 2017;7:8427. doi:10.1038/s41598-017-08670-y

[47] Teske KA, Bogart JW, Arnold LA. Novel VDR antagonists based on the GW0742 scaffold. *Bioorg Med Chem Lett.* 2018;28:351-354. doi: 10.1016/j.bmcl.2017.12.041.

[48] Demizu Y, Takahashi T, Kaneko F, Sato Y, Okuda H, Ochiai E, Horie K, Takagi K, Kakuda S, Takimoto-Kamimura M, Kurihara M. Design, synthesis and X-ray crystallographic study of new nonsecosteroidal vitamin D receptor ligands. *Bioorg Med Chem Lett.* 2011;21:6104-6107. doi: 10.1016/j.bmcl.2011.08.047

[49] Atigadda VR, Brouillette WJ, Duarte F, Babu YS, Bantia S, Chand P, Chu N, Montgomery JA, Walsh DA, Sudbeck E, Finley J, Air GM, Luo M, Laver GW. Hydrophobic benzoic acids as inhibitors of influenza neuraminidase. *Bioorg Med Chem.*

1999;7:2487-2497. doi.org/10.1016/S0968-0896(99)00197-2

[50] Teno N, Yamashita Y, Masuda A, Iguchi Y, Oda K, Fujimori K, Hiramoto T, Nishimaki-Mogami T, Une M, Gohda K. Identification of potent farnesoid X receptor (FXR) antagonist showing favorable PK profile and distribution toward target tissues: Comprehensive understanding of structure-activity relationship of FXR antagonists. *Bioorg Med Chem.* **2019**, 27, 2220-2227, doi:10.1016/j.bmc.2019.04.029.

[51] Mi LZ, Devarakonda S, Harp JM, Han Q, Pellicciari R, Willson TM, Khorasanizadeh S, Rastinejad F. Structural basis for bile acid binding and activation of the nuclear receptor FXR. *Mol Cell*. 2003;11:1093–1100. doi.org/10.1016/S1097-2765(03)00112-6

[52] David TV, Philip S, Dominic S, Anne M, Angela P, Michael RB. Tetrazolium-based assays for cellular viability: a critical examination of selected parameters affecting formazan production. *Cancer Res*. 1991;51:2515-2520. doi: Published May 1991

[53] Hale LV, Galvin RJS, Risteli J, Ma YL, Harvey AK, Yang X, Cain RL, Zeng Q, Frolik CA, Sato M, Schmidt AL, Geiser AG. PINP: A serum biomarker of bone formation in the rat. *Bone*. 2007;40:1103-1109. doi: org/10.1016/j.bone.2006.11.027

[54] Urizar NL, Liverman AB, Dodds DT, Silva FV, Ordentlich P, Yan Y, Gonzalez FJ, Heyman RA, Mangelsdorf DJ, Moore DD. A natural product that lowers cholesterol as an antagonist ligand for FXR. *Science*. 2002;296:1703-1706. doi: 10.1126/science.1072891

[55] Wermuth CG. Selective optimization of side activities: Another way for drug discovery. *J Med Chem*. 2004;46:1303-1014. doi: 10.1021/jm030480f

[56] Carltona DL, Collin-Smith LJ, Daniels AJ, Deaton DN, Goetz AS, Laudeman CP, Littleton TR, Mussod DL, Morgane RJO, Szewczyk JR, Zhang C. Discovery of small molecule agonists for the bombesin receptor subtype 3 (BRS-3) based on an omeprazole lead. *Bioorg Med Chem Lett*. 2008;18:5451-5455. doi: 10.1016/j.bmcl.2008.09.033

Figure caption

Figure 1. Representative FXR agonists with isoxazole derivatives.

Figure 2. Modeling of FXR complexed with GW4064, **19** and **30**. A complex-model of human FXRα-LBD monomer (PDB ID: 3DCT, purple cylinders and orange sticks) with GW4064 (X-ray; yellow sticks) and **19** (left panel, white sticks) and **30** (right panel, white sticks) was built using AutoDock Vina1.1.2.

Figure 3. Effect of **19** on FXR target genes. Expression of FXR-induced genes BSEP, SHP and OSTα was significantly increased by treatment of GW4064 or **19** in Huh-7 cells (n=3, $P < 0.01$ v.s. N.C.)

Figure 4. Selectivity screening of **19** against human nuclear receptors and TGR5. The concentration of ligands for each receptor was as follows; **19**: 1 μM, GW4064: 100 nM, 9-*cis*-retinoic acid (9-*cis*-RA): 50 nM, 1α,25-dihydroxyvitamin D_3 (1,25-OH-VD_3): 100nM, Lithocholic acid (LCA): 200nM, GW7647: 50nM, GW501516: 50nM, GW1929: 50nM, TO901317: 50nM.

Figure 5. Activation of BMP-2-induced osteoblast differentiation by **19** and **30** in ST-2 MSCs. (A) Cell viability. The ST-2 MSCs (vehicle; white columns) were cultured for 12 days in the medium containing 0-10 μM of **19** or **30** (black columns). Cell viability was measured by a WST-8 assay. Cell viability at 0 μM was defined as 100%. Data are presented as means ± S.D.(n=5). (B) ALP staining. The ST-2 MSCs were differentiated into osteoblasts for 12 days in the medium containing BMP-2 (50 ng/ml) together with 10 μM CDCA, 5 μM GW4064, or 1 or 5 μM of **19** or **30** in the presence or absence of 25 μM GS. ALP staining was performed as described in Materials and Methods. The results are the representative from three experiments. (C) ALP activity. The ST-2 MSCs (vehicle: V; white columns) were cultured for 6 or 12 days in the medium containing BMP-2 (50 ng/ml; gray columns) together with one of the FXR agonists, 10 μM CDCA, 5 μM GW4064, and 1 or 5 μM of **19** or **30** (black columns) in the presence or absence of 25 μM GS (hatched columns). Data are shown as means ± S.D.(n=3). *p<0.01, as compared with the BMP-2-induced cells, #p<0.01, as compared with the FXR agonist-treated cells.

Graphical Abstract

N[1]-Substituted benzimidazole scaffold for farnesoid X receptor (FXR) agonists accompanying prominent selectivity against vitamin D receptor (VDR)

Arisa Masuda, Keigo Gohda, Yusuke Iguchi, Ko Fujimori, Yukiko Yamashita, Keisuke Oda, Mizuho Une, Naoki Teno

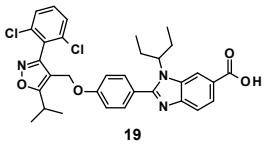

Modeling of FXR complexed with GW4064 and **19**.
A complex-model of human FXRα-LBD monomer (PDB ID: 3DCT, purple cylinders and orange sticks) with GW4064 (X-ray; yellow sticks) and **19** (white sticks) and was built using AutoDock Vina1.1.2.